Available online at www.sciencedirect.com

SCIENCE DIRECT®

Cement and Concrete Research 35 (2005) 562–571

CEMENT AND CONCRETE RESEARCH

Corrosion performance of conventional (ASTM A615) and low-alloy (ASTM A706) reinforcing bars embedded in concrete and exposed to chloride environments

David Trejo[a,*], Paulo J. Monteiro[b]

[a]Department of Civil Engineering, Texas A&M University, 3136 TAMU, College Station, TX 77843, USA
[b]Department of Civil and Environmental Engineering, University of California, 721 Davis Hall, Berkeley, CA 94720, USA

Received 7 April 2003; accepted 3 June2004

Abstract

Conventional reinforcing steel is used in the majority of reinforced concrete structures. In general, steel reinforcement meeting ASTM A615 specifications has been the predominant reinforcement used for these structures. Low-alloy reinforcing steel (ASTM A706) was developed and is being marketed to improve ductility and weldability deficiencies associated with the ASTM A615 reinforcement. Several State Highway Agencies have adopted the use of these low-alloy reinforcing steels. Limited research has been performed on the corrosion characteristics of the steel reinforcement meeting ASTM A706 specifications. This paper presents results from a laboratory study on the critical chloride threshold, macrocell corrosion rates, and mass loss testing for ASTM A706 and ASTM A615 reinforcing steels embedded in concrete and exposed to chloride solution. Results from this study indicate that ASTM A706 reinforcing steel exhibits lower critical chloride threshold levels and higher corrosion rates than ASTM A615 reinforcing steel when embedded in cementitious materials.

Keywords: Corrosion; Chloride; Reinforcement; Transport properties; Concrete

1. Introduction

The effective use of materials in infrastructure systems, especially for corrosion deterioration, must be based on the fundamental understanding of electrochemical thermodynamics and reaction kinetics. Several researchers have provided good overviews on these topics [1–3]. Limited work has been performed on how the microstructural characteristics and surface conditions of reinforcing bars influence the corrosion performance in concrete [4]. The corrosion process of steel reinforcement in concrete typically occurs in two phases, the initiation phase and the propagation phase. The initiation phase is defined as the time from when a structure is placed into service until the time the steel reinforcement begins to corrode. The propagation phase is defined as the time from corrosion initiation to the time when the concrete cover exhibits sufficient cracking or spalling, such that the structure has to be repaired or replaced.

For chloride-induced corrosion, the duration of the initiation phase can be determined using two main variables. The first main variable is the rate of transport of the chloride ions into the concrete towards the steel reinforcement. This variable is dependent on many other variables, including the environment, the concrete characteristics, etc. These variables have been thoroughly investigated and reported throughout the literature [5–10]. Several methods have been proposed to determine the rate at which chloride ions are transported through cementitious materials. This paper will not address the advantages and disadvantages of each method but will only note that several models are available to estimate these chloride transport rates.

The second main variable needed to determine the duration of the initiation phase is the concentration of chloride ions required to initiate corrosion of the steel reinforcement in the concrete environment. This is defined as the critical chloride threshold value. Several researchers have performed research and reported critical chloride threshold values for steel reinforcement embedded in concrete. Thomas [11], Gouda and Halaka [12], and

* Corresponding author. Tel.: +1-979-845-2416; fax: +1-979-845-6554.
E-mail address: trejo@civilmail.tamu.edu (D. Trejo).

0008-8846/$ – see front matter © 2004 Elsevier Ltd. All rights reserved.
doi:10.1016/j.cemconres.2004.06.004

Schiessl and Breit [13] reported critical chloride threshold values from 0.5% to 1.0% by weight of the cement (% wc). Hope and Ip [14] reported values as low as 0.097 % wc, while Gouda and Halaka [12] reported values as high as 3.04 % wc for uncleaned bars. The large variation in these results indicates that there is a significant parameter, or several significant parameters, that influence the critical chloride threshold value of steel reinforcement in concrete. Alonso et al. [15] summarized critical chloride threshold results as a function of test condition, environment, and test method and reported that the critical chloride threshold value is likely not a unique value for all conditions.

Much of the reported work on chloride-induced corrosion mechanisms has focused on nonconcrete environments. It is generally assumed for steels without surface coatings that chloride-induced corrosion results from the breakdown of the passive film. In the presence of a passive film, it is believed that the corrosion process results from the electrostatic attraction between the positively charged metal surface and the negatively charged chloride ions [2]. It is believed that chloride ions react at areas where the passive film is discontinuous, damaged, or at heterogeneous sites on the steel surface. After initiation, the chloride ions are thought to be used as a catalyst for the liberation of iron ions, resulting in further corrosion.

For conventional steel reinforcement, the presence of an iron oxide surface coating (mill scale) formed during the production process makes the presence of a passive film unknown. Very little research has been performed in evaluating the presence of a passive film when mill scale is present. In addition, limited research has been performed to investigate the physical attributes of the mill scale on the steel reinforcement. Fontana [16] did identify the microstructure of iron oxides (mill scale) formed on a steel surface during production as a result of high-temperature oxidation. He reported that a thin layer of hematite (Fe_2O_3) covered a thicker layer of magnetite (Fe_3O_4), which, in turn, covered an even thicker layer of ferrous oxide (FeO), which could be considered to be the passive film. Steel production processes vary, and standard, well-defined mill scales, such as those identified by Fontana [16], are probably not common for steel reinforcing bars.

It has been well established that the formation of passive films is dependent on the chemical composition of the material being used [2,3,17,18]. Conventional reinforcing steels typically do not contain sufficient alloying elements to enhance the stability of the passive film in the presence of chloride ions. Thus, for conventional unalloyed steel reinforcement, the passive films, if present, likely have similar characteristics.

In addition to the mill scale and passive film, the microstructure of the steel could influence the corrosion performance. After the chloride ions penetrate the mill scale or passive film, the microstructure of the steel reinforcement is directly exposed to the chloride ions in the pore solution. Conventional steel reinforcement microstructures typically consist of multiphases of pearlite and ferrite. In general, multiphase microstructures result in higher corrosion activity because these phases generally have marked differences in corrosion performance or because potential differences between the phases lead to localized attack on one phase [19]. Reinforcing steels are typically produced from scrap metal under various environmental conditions. The microstructure of these reinforcing steels varies, depending on the steel composition and production environment. Thus, the production process could influence the corrosion performance of the reinforcement.

The corrosion performance of steel reinforcement embedded in cementitious materials exposed to chlorides is a function of both the concrete and steel characteristics. Critical chloride threshold values and corrosion propagation rates can be influenced by the surface characteristics, the steel composition, and the steel microstructure. This investigation evaluated the critical chloride threshold and corrosion propagation rate of two conventional steel reinforcements (ASTM A615 and A706). The surface conditions, chemistry, and microstructure of each steel type have been evaluated. Because the critical chloride threshold and corrosion rate directly influence the time to first repair, these parameters, or at least a comparison of these parameters, are critical for evaluating the cost effectiveness of the different reinforced concrete systems.

2. Materials, experimental program, and test procedures

The corrosion performance of ASTM A706 reinforcing steel was evaluated and compared with result from ASTM A615 reinforcement using accelerated chloride threshold (ACT) testing and a modified southern exposure (SE) macrocell test. The ACT test method determines the critical chloride threshold of the reinforcement in a mortar environment, while the SE testing evaluates the rate of corrosion propagation of the reinforcing steels in a concrete environment. Both the critical chloride threshold and corrosion rate propagation are needed to estimate the time to first repair of reinforced concrete structures exposed to chlorides.

2.1. Materials

All concrete and mortar mixtures were batched, mixed, and cured in the laboratory. The mortar mixture used for the ACT samples in this study had a water–cement ratio of 0.5. To obtain results within approximately 1 year, the SE samples had a 0.68 water–cement ratio. Type I Ordinary Portland Cement (OPC) meeting specification ASTM C150 was used for both sample types. Ottawa sand meeting specification ASTM C-778 was used for the ACT samples.

Table 1
Mixture proportions for ACT and SE samples

Material	SE samples	ACT samples
	kg/m^3 (lb/cy)	kg/m^3 (lb/cy)
Cement	537 (905)	553 (932)
Water	365 (615)	276 (466)
Fine aggregate	1579 (2661)	1244 (2097)
Coarse aggregate	1388 (2339)	None

The ACT samples contained no course aggregate. The coarse aggregate utilized for the SE concrete samples was 10 mm (3/8 in.) maximum size aggregate (MSA) meeting ASTM C33 specification size number 4. The aggregate was a clean, sound, river gravel, fairly equidimensional in shape. The fine aggregate utilized in the SE concrete samples was a natural, well-graded sand. No mineral or chemical admixtures were incorporated into any of the mixtures used in this study. Table 1 shows the mixture proportions used for the ACT and SE specimens. The slump for the SE samples averaged 100 ± 25 mm (4 ± 1 in.). The unit weight for the ACT mortar samples and SE concrete samples was 2107 (131.4 lb/ft^3) and 2315 kg/m^3 (144.3 lb/ft^3), respectively. All samples were cured for 7 days at 32 ± 3 °C (90 ± 5 °F) and 100% relative humidity.

The steel reinforcing bars for the SE samples were 16-mm (0.63 inch) bars, and the steel reinforcing bars for the ACT samples were 19-mm (0.75 inch) bars. Because the corrosion performance of the reinforcing bars is dependent on the surface conditions, microstructure, and chemical composition, micrographs of the surface mill scale, microstructural analyses (phase identification), and chemical analyses were evaluated for each bar type in this study.

Fig. 1 shows the typical surface characteristics of the steel reinforcing bars. Note the nonuniformity and cracking in the mill scale. Also note that the mill scale has been rolled into the base steel. Fig. 2 shows the microstructure of the bars. Analyses of the microstructure indicated that the ASTM A615 bar consists of approximately 75% pearlite and 25% ferrite. The ferrite phases in the ASTM A615 bars exhibited the presence of residual alloying elements. The A706 bars contained an average of approximately 50% pearlite and 50% ferrite. The ferrite phase in the A706 bars contained less residual alloying elements than did the A615 bars. The average compositions of the reinforcing steels used in the study are shown in Table 2. Both bar types were free of corrosion products prior to casting the samples.

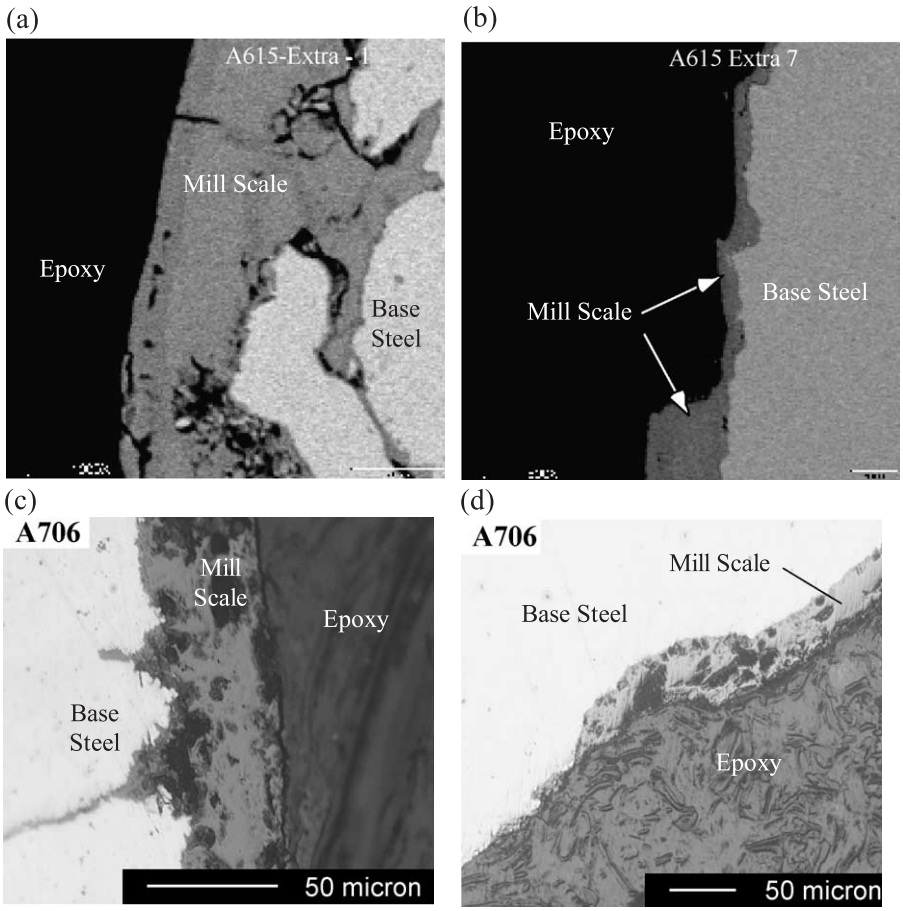

Fig. 1. Cross-sectional micrographs of the surface of steel-reinforcing bars; (a) and (b) ASTM A615; (c) and (d) ASTM A706.

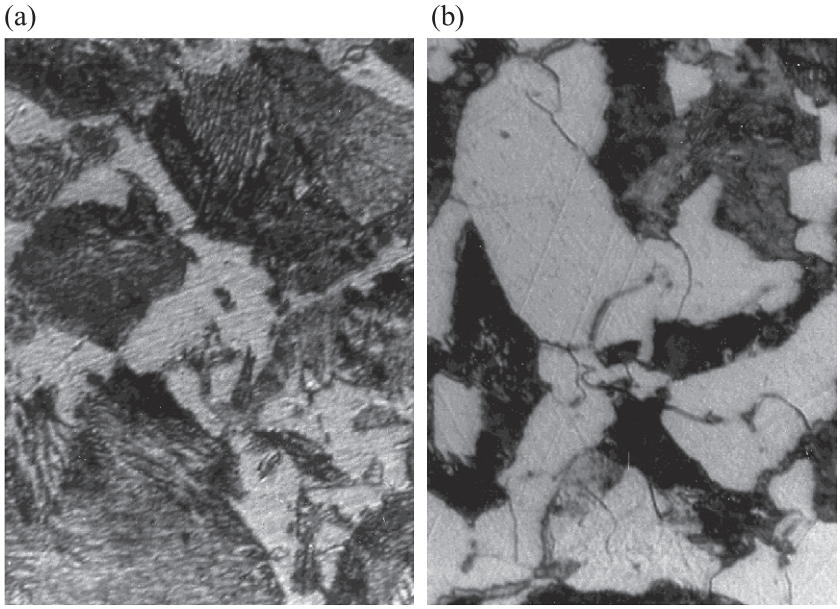

Fig. 2. (a) Optical micrograph of ASTM A615 reinforcing steel. (b) Optical micrograph of ASTM A706 reinforcing steel.

2.2. Experimental program

To determine the critical chloride threshold of the reinforcing steels in plain mortar, a total of 20 ACT samples were fabricated. Ten of these samples contained ASTM A706 reinforcement and 10 contained ASTM A615 reinforcement. One ACT sample containing A706 reinforcing bar broke during testing, and no results were obtained from this sample.

To determine the corrosion propagation rate of the different reinforcing bar types, a total of 20 SE samples were fabricated. Ten of these samples contained ASTM A706 reinforcement and 10 contained ASTM A615 reinforcement. Because ASTM G1 testing was used to determine the mass loss of the reinforcing bars after 1 year, and this test method is a destructive test method, only five samples with each steel type were evaluated and reported for corrosion activity and mass loss. The other five samples were used for other studies.

2.3. Test procedures

Fig. 3 shows the typical layout for the ACT test canister [20]. The test sample is composed of a plastic cylinder used for molding the cementitious material, a chloride transport system for accelerating the chloride ion transport into the cementitious material, and a system for determining the polarization resistance, R_p, of the steel reinforcement embedded in the cementitious material. The R_p is inversely proportional to the corrosion rate.

Table 2
Compositions of steel reinforcement

	C	Mn	P	S	Si	Cu	Ni	Cr	Mo
ASTM A615	0.35	1.04	0.022	0.0445	0.205	0.02	0.21	0.31	0.055
ASTM A706	0.23	0.93	0.0145	0.037	0.22	0.41	0.18	0.18	0.07

The chloride transport system is composed of an anode, a cathode, and an external time-controlled voltage source. The anode in the chloride transport system is a 69-mm-diameter (2.8 in.) Nichrome mesh with a 25×25-mm (1×1 in.) section removed from the center. The cathode in the chloride transport system is a 44-mm-diameter (1.8 inch) Nichrome mesh. The corrosion rate system consists of a standard three-electrode corrosion cell system, a working electrode (the sample being evaluated), a 25×25-mm (1×1 inch) counter electrode, and a saturated calomel reference electrode. A Haber-Luggin probe was used to minimize voltage drops between the reference and working electrodes.

After curing, the samples were removed from the curing room and placed in the laboratory. A potential gradient of 20 V was then applied between the anode and cathode for 12 h each day. The ACT samples with ASTM A615 steel reinforcement had one 12-h potential gradient applied each day for 5 days. Because the ASTM A706 exhibited a lower critical chloride threshold value in the preliminary tests, the ACT samples containing this reinforcement type had a potential gradient applied for 12 h each day for 4 days. After the final 12-h potential gradient was applied, the samples were allowed to rest (no voltage applied) for 42 h. The rest period was immediately followed by evaluating the R_p of the embedded steel reinforcement using a Solartron 1287 potentiostat at a scan rate of 0.0167 mV/s. The scan started at approximately -20 mV from the measured open circuit potential (OCP) and proceeded to approxi-

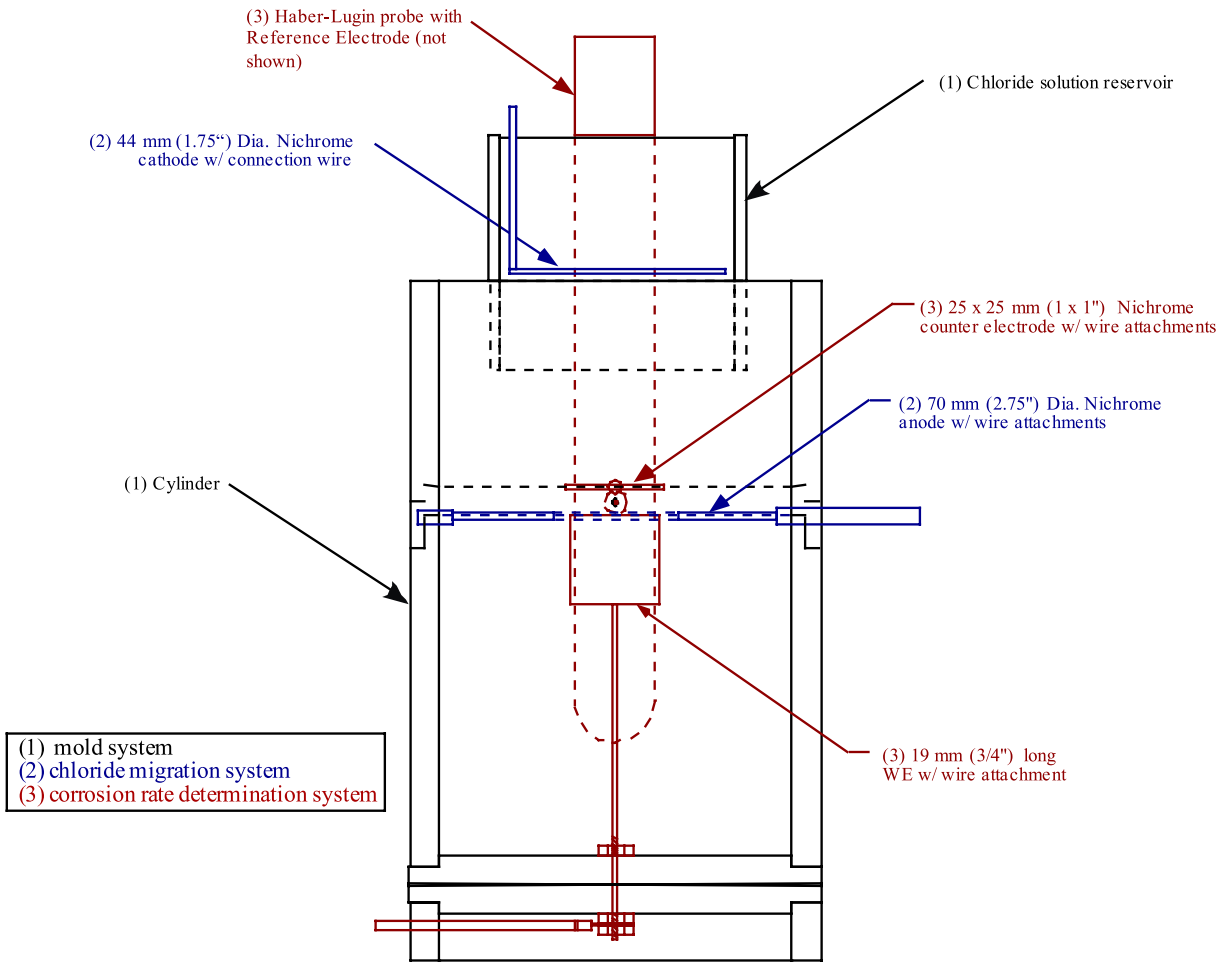

Fig. 3. Layout of ACT test setup.

mately +15 mV from the OCP. IR compensation was used to compensate for the high resistance electrolyte (mortar). After the R_p was evaluated, a 20-V potential gradient was applied between the anode and cathode. It should be noted that the chloride transport system (the anode and cathode) is independent of the working electrode (the steel reinforcing sample being evaluated), and the working electrode is not directly polarized by applying this potential gradient. By not directly applying the potential gradient to the working electrode, changes in the steel–cementitous material interface, which could alter the corrosion performance, are minimized. Trejo and Pillai [20] reported that the application of the voltage resulted in a small reduction in the pH, but this reduction was small and thought to be insignificant for comparison of conventional reinforcing steels.

The R_p value obtained from testing is inversely proportional to the corrosion rate. Therefore, to determine when the steel reinforcement transfers from a passive to active corrosion condition, a best fit line is determined from previous inverse R_p observations. It is assumed that the first several R_p values represent passive conditions because sufficient potential gradients have not been applied to generate chlorides at the steel rebar level. This best fit line provides an estimate for the next inverse R_p value. After the actual inverse R_p value is determined (48 h later), the predicted inverse R_p value is compared with the actual obtained inverse R_p value. If the newly measured inverse R_p value differs significantly from the predicted value, where significantly is defined as a t score of at least 3, the sample is assumed to have transferred from a passive to an active corrosion condition.

After the inverse R_p value indicates that the reinforcement is actively corroding, the specimens are removed from further potential applications, and the chloride ion concentration of the mortar directly adjacent to the steel surface is determined using the modified test method for determining total chloride ion content, as outlined in SHRP-S/FR-92-110 [21]. Because this chloride ion concentration is the chloride ion concentration that initiated the corrosion of the steel reinforcement, it is defined in this paper as the critical chloride threshold value of the steel reinforcement.

Fig. 4 shows the layout for the SE test samples. Macrocell current values were determined by evaluating the voltage across the 10 Ω resistor connecting the top and

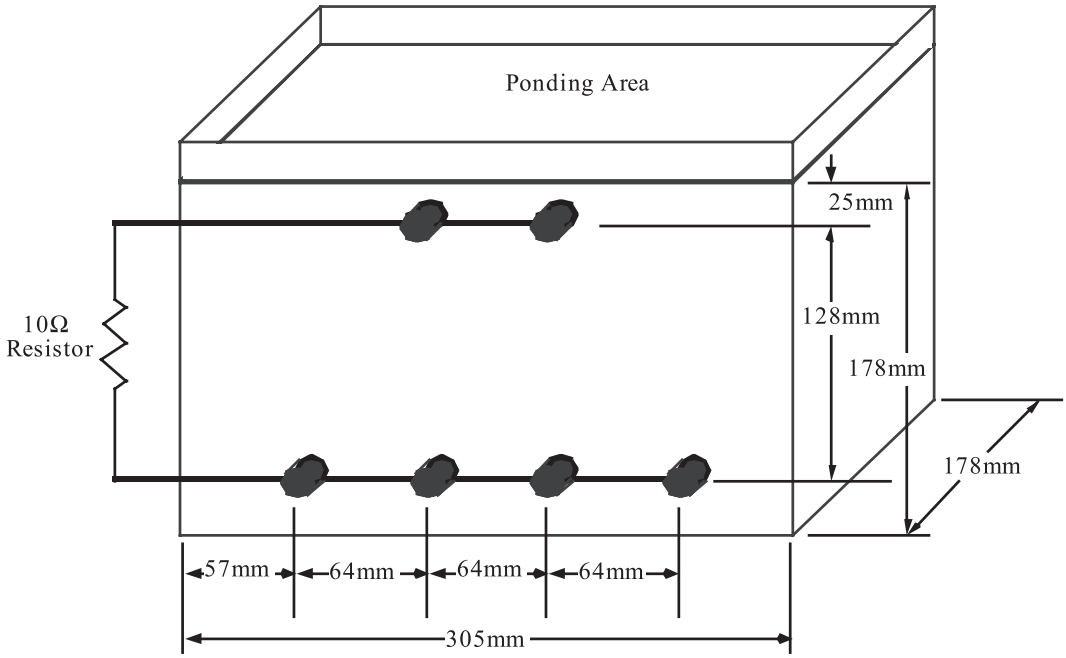

Fig. 4. SE sample layout.

bottom reinforcing mats. The voltage was measured and recorded 5 days per week beginning 14 days (7 days for curing and 7 days for sample preparation) after casting. Alternate wetting and drying cycles were such that the samples were ponded for 7 days, followed by 7 days of drying. The ponding solution was a 3.5 wt.% NaCl solution. The exposure temperature varied between 40 and 45 °C (104 and 113 °F). After 50 weeks of exposure, the mass loss as a result of the macrocell current was calculated by integrating the current as a function of time as shown below:

$$\text{current flow (C)} = \int_0^t I\,\mathrm{d}t \tag{1}$$

where I is the macrocell current and t is time in seconds. Using the current flow value from Eq. (1) and Faradays law, the mass loss resulting from the macrocell current can be determined as follows:

$$\text{mass loss (g)} = \frac{Ita}{nF} \tag{2}$$

where It is the current flow determined from Eq. (1), a is the atomic weight (55.8 amu for iron), n is the number of equivalents exchanged (2 for iron), and F is Faraday's constant (96,500 C/eq). The mean corrosion rate in millimeters per year can be determined using the mass loss as follows:

$$r\left(\frac{\text{mm}}{\text{year}}\right) = 0.00327\left(\frac{ia}{nD}\right) \tag{3}$$

where i is the current density and is defined as current, I, divided by area corroding, A; D is the density of the steel (typically 7.87 g/cm^3), and a and n were defined earlier. This assumes that uniform corrosion occurred over the surface of the steel bars. Observations indicated that only the upper half of the reinforcing bar was corroded. Therefore, only half of the reinforcing bar surface was used to calculate the mean corrosion rates as shown in Eq. (3). Uniform corrosion was assumed for calculation purposes.

Using Eqs. (1)–(3), the SE macrocell results can be evaluated. Because chloride-induced corrosion in concrete is more localized than uniform corrosion is, the authors anticipated that the macrocell current, I, would underestimate the actual current flow and resulting mass loss. As such, reinforcing bars were weighed prior to casting the SE samples, and after the 50 weeks of exposure, the steel reinforcing bar samples were removed from the concrete and evaluated for mass loss using ASTM G1, Standard Practice for Preparing, Cleaning, and Evaluating Corrosion Test Specimens, designation C.3.5. These mass loss data were used to determine the actual mean corrosion rates for the different samples. It should be noted that this mass loss could include the mass loss of the mill scale, resulting in higher corrosion rates. The measured average corrosion rates were then compared with calculated average corrosion rate values determined from the current flow readings. It should be noted that the corrosion rates determined from the SE testing are mean uniform corrosion rates. Because chloride-induced corrosion is often a localized form of corrosion, the assumption of a uniform corrosion rate is not entirely correct. The mean values provide the readers

with a comparative value for the corrosion performance only.

3. Results and discussion

The critical chloride threshold values obtained from the ACT test and the average corrosion rates from the SE tests can provide sufficient information to predict the time to first repair for a reinforced concrete structure. This information can then be used in life-cycle cost assessments to select materials that will provide the owner with the lowest life-cycle costs.

3.1. ACT test results

Table 3 shows the R_p values obtained at different time intervals for the ACT test samples containing ASTM A615 and A706 steel reinforcing bars. The last R_p value reported in Table 3 is the first R_p value that exhibited a t score of at least 3, indicating that the steel reinforcement had transferred from a passive to active state. The chloride ion contents from the mortar adjacent to the steel reinforcement are shown in Table 4. From these data, the average critical chloride threshold for the ASTM A615 steel reinforcement embedded in the mortar is 0.87 kg/m^3 (1.46 lb/cy). The ASTM A706 exhibited an average critical chloride threshold of 0.19 kg/m^3 (0.32 lb/cy).

3.2. SE test results

After 50 weeks of exposure, the SE samples were evaluated for mass loss. Calculated mass loss values were determined using Eqs. (1) and (2). Figs. 5 and 6 show the results from the macrocell testing. Table 5 indicates that the ASTM A706 exhibits a lower calculated average mass loss than the ASTM A615 steel reinforcement does, but with a slightly higher standard deviation. Results from the ASTM G1 mass loss testing, shown in Table 6, clearly show that the mass loss of the ASTM A706 exhibits a higher mass loss than the ASTM A615 reinforcing steel does. The calculated mass loss values are substantially lower than

Table 4
Critical chloride threshold values for ASTM A615 and A706 steel reinforcing bars

Sample identification	Critical chloride concentration threshold value	
	kg/m^3 (lb/cy)	wt.% Cement
A615-1	0.8 (0.5)	0.08
A615-2	0.6 (0.4)	0.07
A615-3[a]	2.3 (1.4)	0.24
A615-4	0.9 (0.6)	0.10
A615-5	0.4 (0.3)	0.05
A615-6	1.5 (0.9)	0.15
A615-7	1.0 (0.6)	0.10
A615-8	0.9 (0.5)	0.10
A615-9	1.1 (0.6)	0.11
A615-10	0.6 (0.3)	0.06
A706-01	0.5 (0.3)	0.06
A706-02	0.6 (0.3)	0.06
A706-03	0.3 (0.2)	0.03
A706-04	0.2 (0.1)	0.02
A706-05	0.3 (0.2)	0.04
A706-06	0.4 (0.2)	0.04
A706-07	0.4 (0.2)	0.04
A706-08	0.3 (0.1)	0.03
A706-09	0.2 (0.1)	0.02

[a] Value is a statistical outlier and was not included in mean value.

Table 3
R_p (Ω/cm^2) values from ACT tests for ASTM A615 and A706 steel reinforcing bars

Sample identification	Total time of applied voltage (h)									
	0	60	66	72	78	84	90	96	102	108
A615-1	5000	11818	3611	10833	10833	5778	4194	3377	1538	
A615-2	2955	4815	4906	6667	4561	1147				
A615-3	3377	7027	10833	19259	13000	7879	1516			
A615-4	6667	6500	3714	6500	4333	3939	728			
A615-5	3939	4561	4981	14943	18571	14444	1775			
A615-6	3939	4194	3939	7027	5532	5652	1135			
A615-7	10400	7222	8125	6190	11304	11818	4194	3611	3562	1044
A615-8	5098	9630	13000	4333	17333	20000	3662	3291	4727	974
A615-9	8667	13000	16250	5306	23636	15294	4000	3467	4214	1728
A615-10	5909	4063	7222	13684	8667	11818	4063	3824	3514	1079
A706-1	13000	26000	13000	4815	2921	7879	6190	1745		
A706-2	15294	14444	14444	6842	6842	18571	5098	3333	1757	
A706-3	6190	7647	8667	4483	3939	4262	3611	1985		
A706-4	3768	5652	7879	4815	6341	2549				
A706-5	7647	10400	12381	8125	11818	2342				
A706-6	12381	5306	11304	9630	4643	2261				
A706-7	11304	5417	10400	8125	4643	2063				
A706-8	13000	4643	13000	7222	15294	2574				
A706-9	11304	6500	7647	4063	4727	2167				

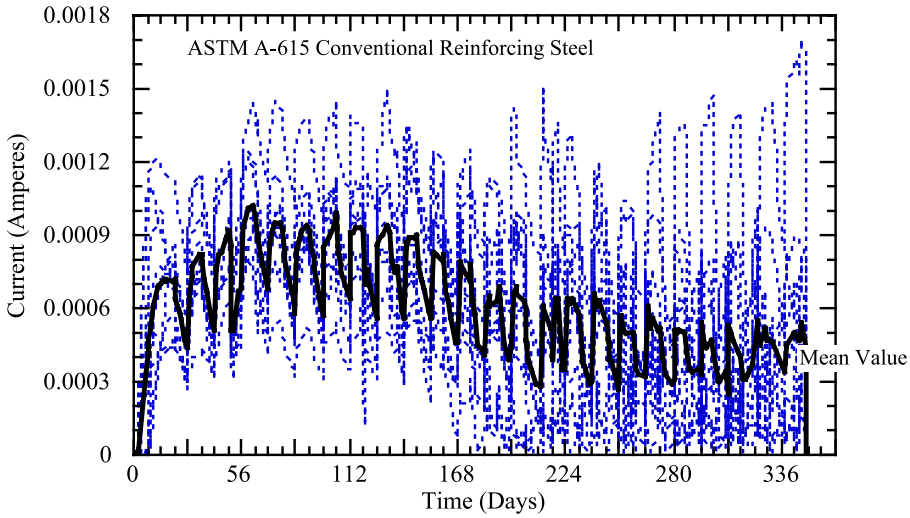

Fig. 5. Macrocell current values from SE specimens with ASTM A615 reinforcing steel.

the actual measured mass loss values. Because chloride-induced corrosion is a relatively localized phenomenon for steel embedded in concrete, it would be expected that localized corrosion cells, where the anode is directly adjacent to the cathode on the same reinforcing bar, would develop. These localized corrosion cells occur in conjunction with the macrocells. The microcells would not be detected by measuring the macrocell current flow between the top and bottom reinforcing bars, and the calculated mass loss values would be less than the measured mass loss values.

For the SE samples containing ASTM A615 steel reinforcing bars, the calculated mass loss only accounted for 33% of the measured mass loss determined from the ASTM G1 testing. For the samples containing ASTM A706 reinforcing bars, the calculated mass loss only accounted for 15% of the measured mass loss. These results indicate that approximately 67% of the overall corrosion in the SE samples containing ASTM A615 reinforcement resulted from microcell corrosion and nearly 85% of the overall corrosion activity in the A706 samples resulted from microcell corrosion. These results also indicate that the reinforcements meeting ASTM A706 specifications evaluated in this work are more susceptible to localized corrosion than the ASTM A615 reinforcement.

Table 7 shows the average corrosion rates for the samples based on the ASTM G1 test results. Results from the five samples indicate that the mean corrosion rate of the ASTM A706 reinforcement, in the aggressive test conditions, is approximately 111 μm/year. The average corrosion rate for the ASTM A615 steel reinforcement is approximately 67 μm/year when exposed and tested under the same environmental conditions. These results indicate that the ASTM A706 exhibits an average corrosion rate 68%

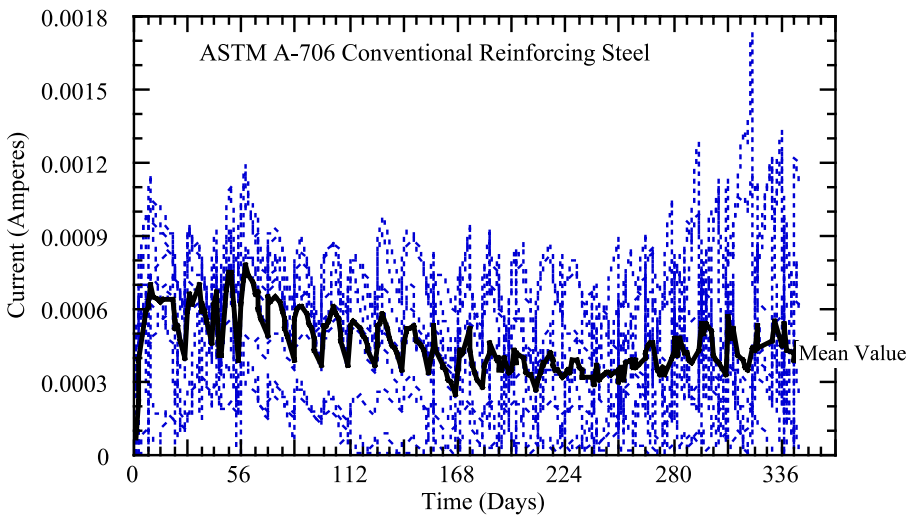

Fig. 6. Macrocell current values from SE specimens with ASTM A706 reinforcing steel.

Table 5
Calculated mass loss values from SE tests

Steel type	Calculated mass loss (%) from macro-cell current flow data						
	Sample 1	Sample 2	Sample 3	Sample 4	Sample 5	Average	S.D.
A-615	0.50	0.74	0.41	0.38	0.78	0.56	0.19
A-706	0.64	0.32	0.56	0.10	0.53	0.43	0.22

higher than the average corrosion rate of the ASTM A615 steel reinforcement.

Because chloride-induced corrosion is a local phenomenon, it is thought that the ASTM A706 reinforcement surface conditions and microstructure enhanced the localized corrosion activity, which would not be detected as a macrocell current flow. Because the morphologies of the mill scales were similar for both steel types investigated and because both steels had little or no constituents that would enhance the protective capacity or stability of the passive film, it is believed that the decrease in corrosion performance is a result of the microstructure characteristics. The potential difference between the ferrite and the pearlite phases in the A706 steel may be larger than the potential difference between the ferrite and the pearlite phases in the A615 steel. This larger potential difference may be a result of the residual elements present in the ferrite phase of the A615 steel. Further studies are needed to validate this finding.

3.3. Performance comparisons

The data from the test program indicates that the critical chloride threshold for the ASTM A615 steel reinforcement is more than four times the critical chloride threshold of the ASTM A706 reinforcement. In addition, the ASTM A615 steel reinforcement exhibited a mean corrosion rate of approximately 60% of the corrosion rate of the ASTM A706 reinforcement. To evaluate the degree of improvement from using the ASTM A615 steel reinforcement, a quantitative assessment will be performed. Although different water–cement ratios and mixture proportions were used for the ACT and SE samples, both test methods indicate that the ASTM A615 steel reinforcement is more resistant to chloride induced corrosion. The following simple analysis is only presented to show the reader that the critical chloride threshold and average corrosion rate are key corrosion performance indicators for predicting the time to repair or service life analyses.

Table 6
Actual mass loss values from SE tests

Steel type	Mass loss (%) data from ASTM G1 testing						
	Sample 1	Sample 2	Sample 3	Sample 4	Sample 5	Average	S.D.
A-615	1.90	1.39	1.99	1.54	1.57	1.68	0.26
A-706	3.90	3.15	1.27	2.83	3.26	2.88	0.98

Table 7
Corrosion rates determined from ASTM G1 tests

Sample no.	Corrosion rate (μm/year)	
	ASTM A615	ASTM A706
1	75	155
2	55	125
3	79	50
4	61	112
5	62	114
Average	67	111

If it is assumed that chloride surface build-up is a function of the square root of time, the solution to Fick's second law is as follows:

$$C(x,t) = k\sqrt{t_o}\left\{\exp^{\left(\frac{-x^2}{4Dt}\right)} - \left(\frac{x\sqrt{\pi}}{\sqrt{4Dt}}\right)\cdot\left(1 - erf\left(\frac{x}{\sqrt{4Dt}}\right)\right)\right\} \quad (4)$$

where x is the concrete cover depth, D is the average diffusion coefficient of the concrete, $C(x,t)$ is the critical chloride threshold value of the reinforcing bar, k is a constant depending on the chloride concentration at the concrete surface, t is the time of exposure in seconds, and t_o is the exposure time in years. If the depth, x, is assumed to be 50 mm, k is 0.3; if D is assumed to be 1.8×10^{-11} m^2/s, and $C(x,t)$ is the critical chloride threshold determined in the research program, the time to corrosion initiation, t, can be determined. Using 0.19 kg/m^3 (0.32 lb/cy) for the critical chloride threshold of ASTM A706 reinforcement, the time to corrosion initiation would be 4.5 years, based on Eq. (4). Using the critical chloride threshold value of the ASTM A615 steel reinforcement, 0.87 kg/m^3 (1.46 lb/cy), the time to corrosion would be 14 years.

To determine the time to first repair, the time required to crack or spall the concrete must also be determined, and this time must be added to the time to corrosion initiation. For diffusion controlled chloride transport, limited work has been performed in determining this time required to crack or spall the concrete cover as a result of corrosion. Pfeifer [22] reported that concrete would crack and spall after 25 μm of the steel reinforcement surface has corroded. Although this is likely not the case for all concrete or mortars, for this example, the time to cracking or spalling will be determined using the relationship reported by Pfeifer as follows [22]:

$$\text{Time to Cracking (years)} = \frac{25\mu\text{m}}{\text{corrosion rate}\left(\frac{\mu\text{m}}{\text{year}}\right)} \quad (5)$$

Using the average corrosion rates determined in this research program, the time to cracking or spalling for the ASTM A615 and A706 reinforcing bars embedded in concrete would be 4.5 and 2.7 months, respectively. These high corrosion rates and short times to cracking are a result

of the high temperatures, high water–cement ratios used for the samples, and the aggressive exposure conditions for the tests. Typically, longer times to cracking or spalling would occur in the field. Using the time to corrosion initiation and the time to cracking, the ASTM A615 reinforcing bars would exhibit a time to repair of approximately 15 years, while the ASTM A706 reinforcing bars would exhibit a time to first repair of approximately 5 years.

4. Conclusions

Critical chloride threshold values and corrosion rates were determined for conventional reinforcing steels meeting ASTM A615 and A706 specifications over a 1-year period. The research program found that the average critical chloride threshold of the ASTM A706 is approximately 0.19 kg/m^3 (0.32 lb/cy). The average critical chloride threshold for the ASTM A615 steel is 0.87 kg/m^3 (1.46 lb/cy), approximately four times that of the ASTM A706 reinforcing bar. The corrosion rates from the SE samples were very high due to the high temperature and aggressive nature of the testing environment and high water–cement ratios used for the SE samples. The average corrosion rate from the SE samples containing ASTM A706 reinforcement was approximately 68% higher than that form the SE samples containing ASTM A615 reinforcement under the same testing conditions. These results indicate that ASTM A706 reinforcing bars are more susceptible to chloride-induced corrosion than ASTM A615 reinforcing bars are, and reinforced concrete structures containing ASTM A615 should exhibit longer times to first repair than structures reinforced with ASTM A706 bars. Based on the material characterization in this program, the reduction in corrosion performance of the ASTM A706 appears to be a result of the microstructure. Further studies are required to confirm and validate these findings.

References

[1] ACI 222R-01, Protection of Metals in Concrete Against Corrosion, American Concrete Institute, Farmington Hills, MI, 2001.
[2] D.A. Jones, Principles and Prevention of Corrosion, 2nd Edition, Macmillan, New York, 1995.
[3] H.H. Uhlig, R.W. Revie, Corrosion and Corrosion Control, 3rd Edition, Wiley, New York, 1985.
[4] D. Trejo, P.J.M. Monteiro, B. Gerwick Jr., G. Thomas, Microstructural design of concrete reinforcing bars for improved performance, ACI Mater. J. 97 (1) (2000) 78–83.
[5] K. Stanish, M. Thomas, The use of bulk diffusion tests to establish time-dependent concrete chloride diffusion coefficients, Cem. Concr. Res. 33 (1) (2003) 55–62.
[6] J.M. Khatib, P.S. Mangat, Influence of high-temperature and low-humidity curing on chloride penetration in blended cement concrete, Cem. Concr. Res. 32 (11) (2002) 1743–1753.
[7] M. Castellote, C. Alonso, C. Andrade, G.A. Chadbourn, C.L. Page, Oxygen and chloride diffusion in cement pastes as a validation of chloride diffusion coefficients obtained by steady-state migration tests, Cem. Concr. Res. 31 (4) (2001) 621–625.
[8] D.M. Roy, W. Jiang, M.R. Silsbee, Chloride diffusion in ordinary, blended, and alkali-activated cement pastes and its relation to other properties, Cem. Concr. Res. 30 (12) (2000) 1879–1884.
[9] N.R. Buenfeld, J.Z. Zhang, Chloride diffusion through surface-treated mortar specimens, Cem. Concr. Res. 28 (5) (1998) 665–674.
[10] A. Delagrave, J. Marchand, E. Samson, Prediction of diffusion coefficients in cement-based materials on the basis of migration experiments, Cem. Concr. Res. 26 (12) (1996) 1831–1842.
[11] M. Thomas, Chloride thresholds in marine concrete, Cem. Concr. Res. 26 (4) (1996) 513–519.
[12] V.K. Gouda, W.Y. Halaka, Corrosion and corrosion inhibition of reinforcing steel, Br. Corr. J. 5 (1970) 204–208.
[13] P. Schiessl, W. Breit, Local repair measures at concrete structures damaged by reinforcement corrosion, in: C.L. Page, P. Bamforth, J.W. Figg (Eds.), Proceedings of the Fourth International Symposium on Corrosion of Reinforcement in Concrete Construction, SCI, Cambridge, 1996, pp. 525–534.
[14] B.B. Hope, A.K. Ip, Chloride corrosion threshold in concrete, ACI Mater. J. 84 (4) (1987) 306–314.
[15] C. Alonso, C. Andrade, M. Castellote, P. Castro, Chloride threshold values to depassivate reinforcing bars embedded in a standardized OPC mortar, Cem. Concr. Res. 30 (7) (2000) 1047–1055.
[16] M.G. Fontana, Corrosion Engineering, Third Edition, McGraw-Hill, New York, 1986.
[17] F. Dabosi, N. Bui, A. Irhzo, Y. Limouzin-Maire, On the mechanism for improved passivation by additions of tungsten to austenitic stainless steels, Corrosion 39 (12) (1983) 491–496.
[18] A.A. Hermas, K. Ogura, S. Takagi, T. Adachi, Effects of alloying Additions on corrosion and passivation behaviors of type 304 stainless steel, Corrosion 51 (1) (1995) 3–10.
[19] NACE, Corrosion Basics—An Introduction, National Association of Corrosion Engineers, Houston, TX, 1984.
[20] D. Trejo, R.G. Pillai, Accelerated chloride threshold testing: Part I. ASTM A615 and A706 reinforcement, ACI Mater. J. 100 (6) (2003) 519–527.
[21] P.D. Cady, E.J. Gannon, Condition Evaluation of Concrete Bridges Relative to Reinforcement Corrosion—Volume 8: Procedural Manual, Strategic Highway Research Program SHRP-S/FR-92-110, National Research Council, Washington, DC, 1992 (September).
[22] D.W. Pfeifer, High performance concrete and reinforcing steel with a 100-year service life, PCI J. 45 (3) (2000) 46–54.